Eur. Phys. J. B **40**, 231–234 (2004)
DOI: 10.1140/epjb/e2004-00275-9

THE EUROPEAN PHYSICAL JOURNAL B

# Optical evidence for the proximity to a spin-density-wave metallic state in $Na_{0.7}CoO_2$

G. Caimi[1], L. Degiorgi[1,a], H. Berger[2], N. Barisic[2], L. Forró[2], and F. Bussy[3]

[1] Laboratorium für Festkörperphysik, ETH Zürich, 8093 Zürich, Switzerland
[2] Institut de physique de la matière complexe (IPMC), EPF Lausanne, 1015 Lausanne, Switzerland
[3] Institute of Mineralogy and Geochemistry, University of Lausanne, 1015 Lausanne, Switzerland

Received 16 May 2004 / Received in final form 6 August 2004
Published online 9 September 2004 – 

**Abstract.** We present the optical properties of $Na_{0.7}CoO_2$ single crystals, measured over a broad spectral range as a function of temperature ($T$). The capability to cover the energy range from the far-infrared up to the ultraviolet allows us to perform reliable Kramers-Kronig transformation, in order to obtain the absorption spectrum (i.e., the complex optical conductivity). To the complex optical conductivity we apply the generalized Drude model, extracting the frequency dependence of the scattering rate ($\Gamma$) and effective mass ($m^*$) of the itinerant charge carriers. We find that $\Gamma(\omega) \sim \omega$ at low temperatures and for $\omega > T$. This suggests that $Na_{0.7}CoO_2$ is at the verge of a spin-density-wave metallic phase.

**PACS.** 78.20.-e Optical properties of bulk materials and thin films – 74.70.Dd Ternary, quaternary and multinary compounds (including Chevrel phases, borocarbides, etc.) – 75.30.Fv Spin-density waves

Rapid Note

The discovery of superconductivity at 5 K in hydrated sodium cobaltate [1] has attracted considerable attention. How water inclusion triggers superconductivity in $Na_xCoO_2$ is not fully understood yet. The investigation of non-hydrated sample is therefore of relevance and a considerable research effort has been devoted to $Na_xCoO_2$ specimens with $x$ ranging between 0.3 and 0.75. As $x$ increases from 0.3, the ground state goes from a paramagnetic metal to a charge-ordered insulator for $x = 0.5$ to a Curie-Weiss metal around 0.7 and finally to a weak-moment magnetically ordered state for $x > 0.75$ (Ref. [2]). This latter phase is supposed to be equivalent to a so called spin-density-wave (SDW) metal. Several recent investigations [3–5], based on magnetic, thermal and transport properties as well as muon spin spectroscopy, indicate the formation of a SDW metallic state for $x = 0.75$.

Optical experiments are well-known tools in order to achieve information about the electrodynamic response of the investigated system, and to shed light on its electronic structure. From the absorption spectrum one can also extract the effective mass and the scattering rate of the itinerant charge carriers. Lupi et al. measured the optical conductivity of $Na_xCoO_2$ (for $x = 0.57$) and reported an "anomalous Drude" behavior, where the charge carrier have an effective mass of $5m_b$ and their scattering rate is $\Gamma(\omega) = \frac{1}{\tau(\omega)} \sim \omega^{3/2}$ (Ref. [6]). Wang et al. optically investigated $Na_{0.7}CoO_2$, mainly focusing their attention on the high frequency spectral range. They found two broad interband transitions at 1.6 eV and 3.2 eV ascribed to the $t_{2g} - e_g$ band transitions by invoking the effect of the exchange splitting [7]. Additionally, a mid-infrared peak at about 0.4 eV was attributed to interband transition within the $t_{2g}$ manifold or to the electronic correlation effect. At lower frequencies a non simple Drude intraband response was detected, as well [7].

In this short communication, we offer our optical investigations on high quality $Na_{0.7}CoO_2$ single crystals. Our specimens have a size $2 \times 2$ mm and were grown by the flux methods as thoroughly described elsewhere [8]. X-ray scattering measurements on these crystals attest the Na content to $0.700 \pm 0.016$. Samples from the same batch were furthermore characterized by the dc transport measurements [9]. The temperature dependence of the resistivity $\rho(T)$ (inset of Fig. 1b) within the $ab$ plane displays a linear behavior in temperature from 300 down to 100 K, as well as below 100 K, however with a smaller slope, in agreement with data of references [2] and [10]. We performed optical reflectivity measurements from the far-infrared (FIR) up to the ultraviolet (i.e., 5 meV – 12.4 eV) as a function of temperature between 10 and 300 K. Measurements were performed also in a magnetic field up to 7 T. No changes in the spectra were however found as a function of field. Our investigations covers the largest spectral range addressed so far on $Na_xCoO_2$. Details pertaining the experiments can be found elsewhere [11,12].

Figure 1a displays the optical reflectivity R($\omega$). Beside some absorptions at about and above 1 eV, one can recognize the quite sharp plasma edge feature with

[a] e-mail: degiorgi@solid.phys.ethz.ch

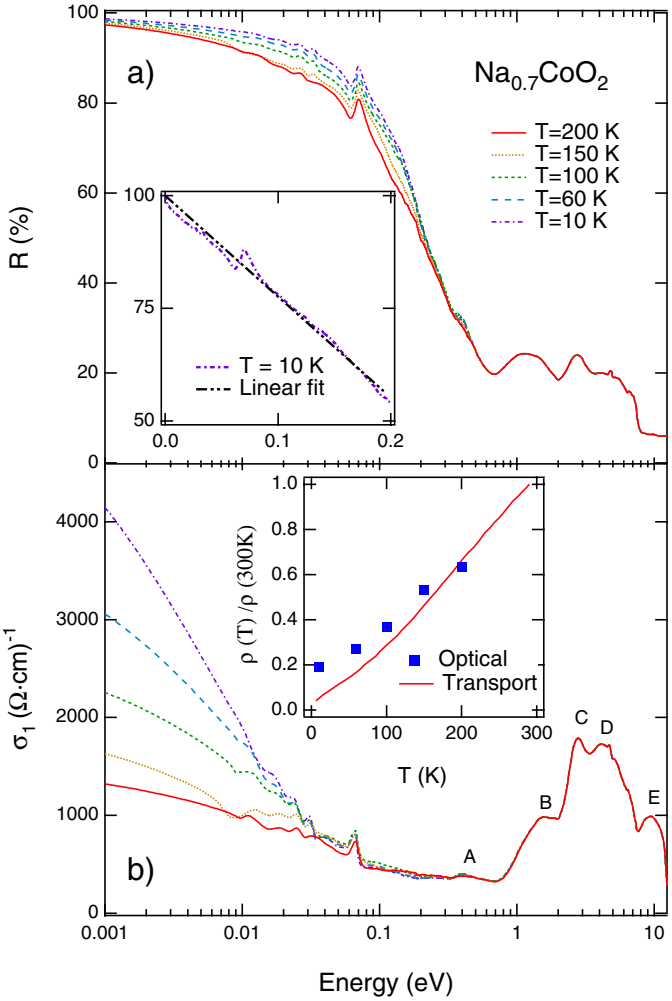


**Fig. 1.** (Color online) a) Reflectivity and b) real part $\sigma_1(\omega)$ of the optical conductivity of $Na_{0.7}CoO_2$ at selected temperatures. The four high frequency absorptions in $\sigma_1(\omega)$ are labeled (see text). Inset a): R($\omega$) at 10 K between 0 and 0.2 eV, emphasizing the linear behavior of R($\omega$) at low energies. Inset b): Comparison of $\rho_{dc}(T)$ and the estimation of the dc resistivity from the optical experiment (i.e., $\rho_{dc}^{optical}(T) = 1/\sigma_1(\omega \to 0, T)$)(Figure available in color at `http://www.eurphysj.org`).

onset at ≃0.7 eV. R($\omega$) increases with decreasing temperature below 0.2 eV, indicative for the metallic character of $Na_{0.7}CoO_2$. Furthermore, we clearly see at 0.07 eV the infrared-active phonon mode. Our data bears an overall similarity with the finding of Lupi et al. for $Na_{0.57}CoO_2$ (Ref. [6]). There is also a rough agreement with the optical response measured on $Na_{0.7}CoO_2$ by Wang et al. [7]. In this latter data, there is a crossing of the R($\omega$) spectra around 0.1 eV and the formation of a bump at about 0.03 eV with decreasing temperature, for which neither our spectra nor those of Lupi et al. give a clear cut evidence.

The real part $\sigma_1(\omega)$ of the optical conductivity, shown in Figure 1b, is obtained through Kramers-Kronig (KK) transformations of R($\omega$). We have extrapolated the R($\omega$) spectra towards zero energies with the Hagen-Rubens extrapolation [11,12], using dc values of the conductivity in agreement with the transport results [2,5,10]. The good agreement between $\sigma_1(\omega \to 0)$ and $\sigma_{dc} = \frac{1}{\rho_{dc}}$ is emphasized by the inset in Figure 1b, supporting furthermore the validity of the KK procedure. Standard extrapolation of $R(\omega) \sim \omega^{-s}$ (with $2 < s < 4$) were employed at high frequencies. It is easy verified that the main conclusions of our work are fully independent from the employed extrapolations due to the extremely broad measured spectral range. As expected from the R($\omega$) spectra, the effective intraband metallic component in $\sigma_1(\omega)$ is enhanced below 0.03 eV and the $\sigma_1(\omega \to 0)$ limit increases with decreasing temperature, as typical for a metallic system. At higher frequencies we recognize a weak feature at 0.4 eV (A) followed by more pronounced and well defined features at 1.4 eV (B), at 2.8 eV (C), at 4.8 eV (D), and at 10 eV (E). These latter absorptions are in fair agreement with the data of Wang et al. [7] and in good accord with the recent findings obtained with the ellipsometry method [13]. Furthermore, angle resolved photoemission results identify electronic excitations at 0.7, 3, 4.1, 6 and 11 eV (Ref. [14]). In passing, we note that some of the detected absorptions could be ascribed to electronic interband transitions involving the Co 3$d$ $t_{2g}$ and $e_g$ manifolds and their exchange splitting [15,16].

The metallic component of $\sigma_1(\omega)$ cannot be fully reproduced by a simple Drude term, the most common description for simple metals, also successfully applied in several oxides. The effective metallic component of the optical conductivity can be alternatively described in terms of an "anomalous or generalized Drude" model [6], where both the effective mass $m^*(\omega)/m_b$ and the scattering rate $\Gamma(\omega)$ of the itinerant charge carriers are allowed to depend on frequency. We analyze the complex optical conductivity $\tilde{\sigma}(\omega) = \sigma_1(\omega) + i\sigma_2(\omega)$, obtained through KK analysis, by applying the following expression [17]:

$$\tilde{\sigma}(\omega) = \tilde{\sigma}_D(\omega) + \frac{i\omega}{4\pi}(\epsilon_\infty - 1) \qquad (1)$$

where:

$$\tilde{\sigma}_D(\omega) = \sigma_{1D}(\omega) + i\sigma_{2D}(\omega) = \frac{\omega_p^2}{4\pi}\frac{1}{\Gamma(\omega) - i\omega\frac{m^*(\omega)}{m_b}} \qquad (2)$$

is the generalized Drude component and $\epsilon_\infty$ is the optical dielectric constant. By inverting equation (2) we obtain:

$$\Gamma(\omega) = \frac{\omega_p^2}{4\pi}\frac{\sigma_{1D}}{|\sigma_D|^2} \qquad (3)$$

$$\frac{m^*(\omega)}{m_b} = \frac{\omega_p^2}{4\pi}\frac{\sigma_{2D}}{\omega|\sigma_D|^2} \qquad (4)$$

In practice, we use the experimental $\tilde{\sigma}(\omega)$ in order to evaluate the frequency dependence of the effective mass and scattering rate. $\omega_p^2$ is the spectral weight associated with the itinerant charge carriers, and it can be estimated by integrating $\sigma_1(\omega)$ from zero frequency up to a cut-off frequency $\omega_c$ coinciding with onset of electronic interband transitions. We choose $\omega_c \approx 0.63$ eV, giving a value of

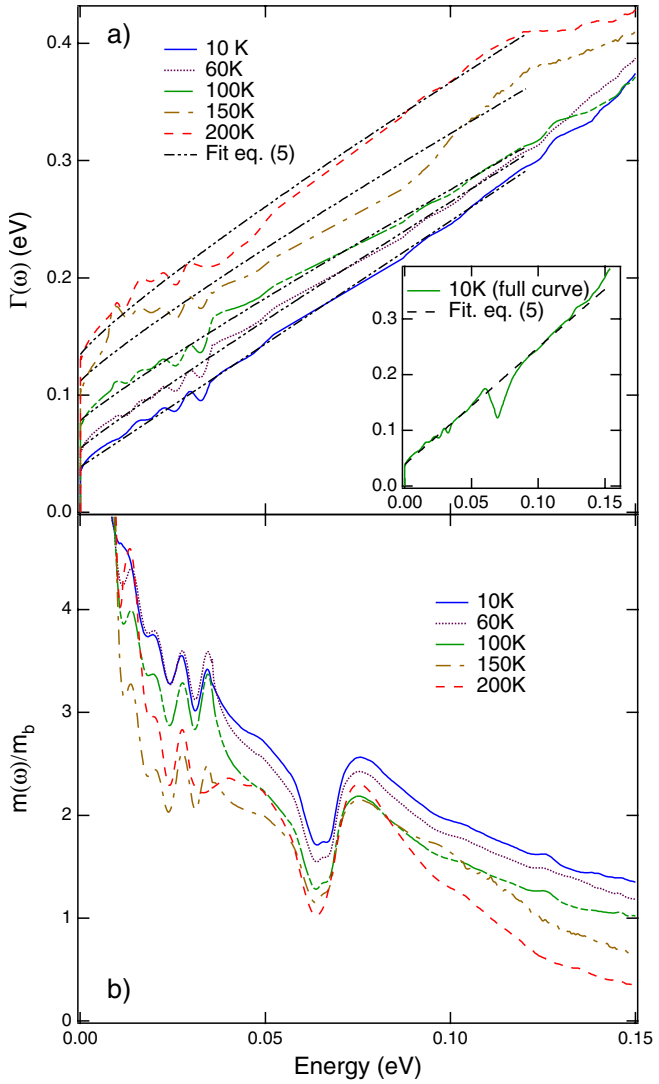


**Fig. 2.** (Color online) a) Frequency dependence of the scattering rate (Eq. (3)) and its fit according to equation (5) at selected temperatures. Note that the IR active phonon has been subtracted in order to better highlight the linear or sub-linear fit. Inset: the original curve of $\Gamma(\omega)$ (i.e., comprehensive of the IR phonon at 0.07 eV) at 10 K is shown with the fit after equation (5) with $\alpha = 1$. The phonon subtraction does not affect the fit of $\Gamma(\omega)$. This is true at all temperatures. b) Frequency dependence of $m^*(\omega)/m_b$ at selected temperatures (Eq. (4)) (Figure available in color at `http://www.eurphysj.org`).

$\omega_p \simeq 1.17$ eV. The $\epsilon_\infty$ constant corresponds to the value of the real part ($\epsilon_1(\omega)$) of the dielectric function at $\omega \simeq \omega_c$; namely, $\epsilon_\infty = 3.75$. Figure 2a displays the frequency dependence of the scattering rate $\Gamma$ below 0.15 eV. For clarity, the depletion of $\Gamma(\omega)$ at 0.07 eV, due to the phonon mode, has been removed from the data (see below). Moreover, $m^*(\omega)/m_b$ (Fig. 2b) weakly increases with decreasing frequency at all temperatures, reaching a value of about 5 in the limit $\omega \to 0$. This agrees with Lupi's data [6].

As expected, $\Gamma(\omega)$ decreases with decreasing temperature. Over a very broad spectral range, extending up to about 0.12 eV, $\Gamma(\omega)$ can be fitted with the power law

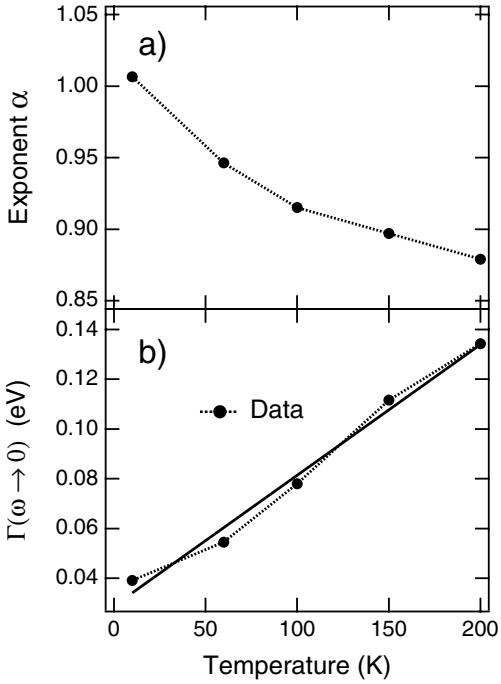


**Fig. 3.** a) Temperature dependence of the exponent $\alpha$ in equation (5). b) Temperature dependence of $\Gamma(\omega)$ in the static limit $\omega \to 0$. $\Gamma(\omega \to 0)$ can be well approximated by a linear fit.

expression:

$$\Gamma(\omega) \sim \omega^\alpha. \tag{5}$$

We establish that $\alpha \simeq 1$ for temperatures below about 50 K. $\Gamma(\omega) \sim \omega$ might be indicative of a non-Fermi liquid behavior in $Na_{0.7}CoO_2$. The exponent $\alpha$ (Fig. 3a) tends nevertheless to decrease at higher temperatures (e.g., $\alpha = 0.88$ at 200 K). We emphasize at this point that our fit after equation (5) is not affected by the ad-hoc phonon subtraction. The inset of Figure 2 shows indeed that even the original curve of $\Gamma(\omega)$ at 10 K can be well fitted by equation (5) with $\alpha = 1$. The same applies for all temperatures, making our analysis of $\Gamma(\omega)$ robust. The linear frequency dependence of $\Gamma(\omega)$ at $\omega > T$ pairs with the linear temperature dependence of $\rho_{dc}(T)$ for $T < 100$ K in the compound with 71% Na content [2,9].

Ruvalds and Virosztek proposed a while ago a Fermi-surface nesting scenario for describing the optical properties of superconducting oxides [18]. They showed that Fermi-surface nesting modifies the electron-electron scattering and therefore yields an unusual variation of the optical reflectivity. Within this scenario, also applicable for the charge- and spin-density-wave state where nesting is an essential ingredient [18], the effective Drude component is characterized by a relaxation rate that is linear in frequency for $\omega > T$ (Fig. 2a). Ruvalds and Virosztek [18] also predicts that $\Gamma(\omega \to 0) \sim T$, as verified in Figure 3b, where $\Gamma(\omega)$ in the static limit $\omega \to 0$ as a function of $T$ is shown. Furthermore, R($\omega$) is linear in $\omega$ in a broad spectral range (inset of Fig. 1a), in agreement with the theory [18]. Our findings in $Na_{0.7}CoO_2$ support the Fermi-surface nesting scenario. Consequently, considering

the phase diagram reported in reference [2], we can affirm that $Na_{0.7}CoO_2$ seems to be at the verge of a SDW metallic phase. The linear frequency dependence of $\Gamma(\omega)$ at low temperatures differs from the conclusion of Lupi et al. on $Na_{0.57}CoO_2$, for which $\alpha \simeq 3/2$ (Ref. [6]). This could be explained by the different stoichiometry of the samples. $Na_{0.57}CoO_2$ is quite close to the charge-ordered insulating boundary (at $x = 0.5$) between a paramagnetic metal and a Curie-Weiss metal [2]. On the contrary, our sample $Na_{0.7}CoO_2$ is located in the phase diagram [2] well within the Curie-Weiss metal sector and is close to the boundary (at least for low temperatures) of the SDW metallic phase. We shall finally note that after reference [18] a non Fermi liquid-Fermi liquid crossover is not excluded at very low temperatures in the case of an imperfect Fermi-surface nesting. This would be in agreement with the dc-transport data on $Na_{0.7}CoO_2$. Indeed for $T < 1$ K, $\rho(T)$ displays a typical Fermi liquid $T^2$ behavior [19].

In conclusion, we have provided the complete absorption spectrum of $Na_{0.7}CoO_2$. The frequency dependence of the scattering rate of the itinerant charge carriers is extracted from the complex optical conductivity, and we have established that $\Gamma(\omega) \sim \omega$ at low temperatures. $Na_{0.7}CoO_2$ seems to be in the proximity of a spin-density-wave metallic state. It turns out [2] that the exact stoichiometry plays an essential role in defining the intrinsic physical properties of $Na_xCoO_2$. As future outlook, we wish to fine tuning the Na content $x$ between 0.7 and 0.85 and study the corresponding optical response. The SDW metallic phase for $x > 0.7$ is an appealing scenario, supported by experimental and theoretical results [20,21], but might be not the unique one. Interestingly enough, Bernhard et al. [13] found evidence for a polaronic band in the case of $x = 0.82$.

The authors wish to thank J. Müller for technical help and A. Perucchi for fruitful discussions. This work has been supported by the Swiss National Foundation for the Scientific Research.

## References

1. K. Takada, H. Sakurai, E. Takayama-Muromachi, F. Izumi, R.A. Dilanian, T. Sasaki, Nature **422**, 53 (2003)
2. M.L. Foo, Y. Wang, S. Watauchi, H.W. Zandbergen, T. He, R.J. Cava, N.P. Ong, Phys. Rev. Lett. **92**, 247001 (2004)
3. B.C. Sales, R. Jin, K.A. Affholter, P. Khalifah, G.M. Veith, D. Mandrus, submitted to Phys. Rev. B, `cond-mat/0402379`
4. J. Sugiyama, J.H. Brewer, E.J. Ansaldo, B. Hitti, M. Mikami, Y. Mori, T. Sasaki, Phys. Rev. B **69**, 214423 (2004)
5. T. Motohashi, R. Ueda, E. Naujalis, T. Tojo, I. Terasaki, T. Atake, M. Karppinen, H. Yamauchi, Phys. Rev. B **67**, 064406 (2003)
6. S. Lupi, M. Ortolani, P. Calvani, Phys. Rev. B **69**, 180506 (2004)
7. N.L. Wang, P. Zheng, D. Wu, Y.C. Ma, T. Xiang, R.Y. Jin, D. Mandrus, `cond-mat/0312630`
8. M.N. Iliev, A.P. Litvinchuk, R.L. Meng, Y. Sun, J. Cmaidalka, C.W. Chu, Physica C **402**, 239 (2004)
9. The dc resistivity $\rho(T)$ was measured within the *ab* plane and along the *c*-axis at EPF-Lausanne, with the conventional four points contact method
10. Y. Wang, N.S. Rogado, R.J. Cava, N.P. Ong, Nature **423**, 425 (2003)
11. F. Wooten, *Optical Properties of Solids* (Academic Press, New York, 1972)
12. M. Dressel, G. Grüner, *Electrodynamics of Solids* (Cambridge University Press, Cambridge, 2002)
13. C. Bernhard, A.V. Boris, N.N. Kovaleva, G. Khaliullin, A. Pimenov, L. Yu, D.P. Chen, C.T. Lin, B. Keimer, `cond-mat/0403155`
14. M.Z. Hasan, Y.-D. Chuang, D. Qian, Y.W. Li, Y. Kong, A. Kuprin, A.V. Fedorov, R. Kimmerling, E. Rotenberg, K. Rossnagel, Z. Hussain, H. Koh, N.S. Rogado, M.L. Foo, R.J. Cava, Phys. Rev. Lett. **92**, 246402 (2004)
15. D.J. Singh, Phys. Rev. B **61**, 13397 (2000)
16. K.W. Lee, J. Kunes, W.E. Pickett, Phys. Rev. B **70**, 045104 (2004); `cond-mat/0308388`
17. J. Hwang, T. Timusk, G.D. Gu, Nature **427**, 714 (2004)
18. J. Ruvalds, A. Virosztek, Phys. Rev. B **43**, 5498 (1991)
19. S.Y. Li, L. Taillefer, D.G. Hawthorn, M.A. Tanatar, J. Paglione, M. Sutherland, R.W. Hill, C.H. Wang, X.H. Chen, Phys. Rev. Lett. **93**, 056401 (2004)
20. M.D. Johannes, I.I. Mazin, D.J. Singh, D.A. Papaconstantopoulos, `cond-mat/0403135`
21. J. Wooldridge, D.M. Paul, G. Balakrishnan, M.R. Lees, submitted to J. Phys.: Condens. Matter, `cond-mat/0406513`